

RESEARCH ARTICLE

Open Access

Single-cell analysis of nasal epithelial cell development in domestic pigs



Wenqian Wang¹, Ruiling Liu¹, Qiu Zhong¹, Yunlei Cao¹, Jiaxin Qi¹, Yuchen Li^{1*} and Qian Yang^{1*} 

Abstract

The nasal mucosa forms a critical barrier against the invasion of respiratory pathogens. Composed of a heterogeneous assortment of cell types, the nasal mucosa relies on the unique characteristics and complex intercellular dynamics of these cells to maintain their structural integrity and functional efficacy. In this study, single-cell RNA sequencing (scRNA-seq) of porcine nasal mucosa was performed, and nineteen distinct nasal cell types, including nine epithelial cell types, five stromal cell types, and five immune cell types, were identified. The distribution patterns of three representative types of epithelial cells (basal cells, goblet cells, and ciliated cells) were subsequently detected by immunofluorescence. We conducted a comparative analysis of these data with published human single-cell data, revealing consistent differentiation trajectories among porcine and human nasal epithelial cells. Specifically, basal cells serve as the initial stage in the differentiation process of nasal epithelial cells, which then epithelial cells. This research not only enhances our understanding of the composition and transcriptional signature of porcine nasal mucosal cells but also offers a theoretical foundation for developing alternative models for human respiratory diseases.

Keywords Nasal epithelial cells, ScRNA-seq, cross-species comparison, respiratory virus receptors

Introduction

Recurrent outbreaks of respiratory infectious diseases have had a significant economic impact on the global swine industry [1]. Given that the nasal cavity serves as a primary entry point for pathogens, enhancing nasal mucosal barrier function is critically important for the effective prevention of respiratory infectious diseases [2]. A comprehensive comprehension of the fundamental organization and cellular composition of the nasal mucosa is essential for developing effective strategies to augment the functionality of the nasal mucosal barrier. However, owing to the limitations of available

techniques, the study of the nasal cavity has traditionally relied on histomorphology analysis, resulting in a dearth of comprehensive knowledge on the specific cellular composition and interactions within the nasal cavity [3–5]. Single-cell RNA sequencing represents a groundbreaking tool for examining heterogeneous cell populations [6] and has been employed to construct single-cell transcriptome atlases of significant tissues in humans and diverse mammals [7, 8]. Although single-cell atlases of more than 20 porcine tissues have been constructed [9], single-cell atlases from the porcine nasal cavity have yet to be reported.

Owing to their genetic, anatomical, physiological, and immunological similarities with humans, domestic pigs are recognized as critical biomedical models for the study of human diseases [10–13]. They have been extensively utilized in research on various conditions, such as atherosclerosis [14], diabetes [15], and heart disease [16], and have even facilitated the development of porcine kidneys for human xenotransplantation [17]. Multiple studies have revealed that human respiratory viruses, including

Communicated by Vincent Béringue.

*Correspondence:

Yuchen Li

yuchenli2022@njau.edu.cn

Qian Yang

zxbyq@njau.edu.cn

¹ Present Address: MOE Joint International Research Laboratory of Animal Health and Food Safety, College of Veterinary Medicine, Nanjing Agricultural University, Nanjing, Jiangsu, China



© The Author(s) 2024. **Open Access** This article is licensed under a Creative Commons Attribution 4.0 International License, which permits use, sharing, adaptation, distribution and reproduction in any medium or format, as long as you give appropriate credit to the original author(s) and the source, provide a link to the Creative Commons licence, and indicate if changes were made. The images or other third party material in this article are included in the article's Creative Commons licence, unless indicated otherwise in a credit line to the material. If material is not included in the article's Creative Commons licence and your intended use is not permitted by statutory regulation or exceeds the permitted use, you will need to obtain permission directly from the copyright holder. To view a copy of this licence, visit <http://creativecommons.org/licenses/by/4.0/>. The Creative Commons Public Domain Dedication waiver (<http://creativecommons.org/publicdomain/zero/1.0/>) applies to the data made available in this article, unless otherwise stated in a credit line to the data.

influenza A virus (IAV) and severe acute respiratory syndrome coronavirus (SARS-CoV), exhibit similar infectious and pathogenic characteristics in pigs [18, 19]. Recently, numerous studies have successfully utilized pigs or cultured porcine respiratory tract tissues to elucidate the infection dynamics and pathogenic mechanisms of various human respiratory viruses [20, 21], which suggests that the porcine nasal cavity is an effective alternative model for human respiratory disease research. Thus, exploring the characteristics of porcine and human nasal mucosa at the cellular and molecular levels warrants further investigation.

In this study, we constructed a single-cell atlas of porcine nasal mucosa and performed a comparative analysis with human single-cell data. We investigated the composition, differentiation trajectories, and intercellular communication of nasal mucosal cells in both pigs and humans. Moreover, we analysed the transcriptional characteristics of cell–cell junction molecules, pattern recognition receptors (PRRs), and various respiratory virus receptors. This research not only reveals the characteristics of porcine nasal mucosa cells but also offers new insights into the development of alternative porcine nasal models for human respiratory diseases.

Materials and methods

Animals

Conventional Duroc × (Landrace × Yorkshire) neonatal piglets (5 days old) were obtained from the Jiangsu Academy of Agricultural Science. All the piglets were seronegative for antibodies against porcine epidemic diarrhea virus, porcine reproductive and respiratory syndrome, transmissible gastroenteritis virus, influenza A virus and porcine circovirus type 2. The animal studies were approved by the Institutional Animal Care and Use Committee of Nanjing Agricultural University and followed the National Institutes of Health guidelines for the performance of animal experiments.

Cell isolation and single-cell sequencing

Single-cell capture was performed using a Chromium Controller instrument (10× Genomics) as previously described [22]. The mucosa of the nasal respiratory region was dissected from four 5-day-old piglets (two porcine nasal mucosae were mixed into one sample) [5] and then cut into small pieces, which were digested with collagenase type IV (4 mg/mL, Miltenyi Biotec) and hyaluronidase (0.25 mg/mL, Miltenyi Biotec) for 30 min at 37 °C. The released nasal cells were filtered through a 70 µm cell strainer, centrifuged and resuspended in PBS. The activity of the suspended cells was determined by trypan blue staining, and the live cell concentration was adjusted to 1000–2000 cells per microliter. The cells were

then captured with a 10× Genomics Chromium Single Cell Instrument after binding to barcoded gel beads. The raw scRNA-seq data were obtained after reverse transcription and RNA sequencing. These processes were completed by Gene Denovo (Guangzhou, China).

Single-cell RNA sequencing data processing and clustering analysis

The raw sequencing data were processed by using 10X Genomics Cell Ranger software (version 3.1.0, USA), and the sequence reads were aligned to the porcine reference genome Sscrofa 11.1. Single-cell analysis was performed using the Seurat v3 [23]. Cells with fewer than 200 or more than 6500 detected genes were excluded. Cells with unusually high numbers of unique molecular identifiers (UMIs) ($\geq 50\,000$) or mitochondrial gene percentages ($\geq 15\%$) were excluded. Moreover, gel bead-in-emulsion (GEM) mixtures carrying multiple cells were also filtered out. After high-quality cells were retained, we employed the log normalization method to normalize gene expression. To minimize the effects of behavioral conditions and batch variability on clustering, we used Harmony [24] to cluster the data in which the cells were grouped by cell type. Then, principal component analysis (PCA) was used to scale and dimensionally reduce the resulting integrated expression matrix. We used Seurat, which implements a graph-based clustering approach, to cluster the cells. For visualization of clusters, t-distributed stochastic neighbor embedding (t-SNE) was generated using the same PC. Finally, we loaded the log-normalized matrices on the SingleR package for cell type annotation.

Single-cell RNA sequencing data integration

To integrate our data with published human nasal single-cell RNA sequencing data (including nasal biopsies from three adults and nasal brushings from four adults) [7], we adopted the R package Seurat, and integration was performed as previously reported [25]. The Ensembl genome browser (Ensembl-release 106) was used to convert human (GRCh38) gene names to the corresponding pig gene names before integration. For this analysis, only genes with one-to-one orthologues were utilized, ensuring high quality and consistency. Low-quality cells and genes were excluded from the dataset. Each dataset underwent independent normalization before identifying the features with the highest variability. A standard integration workflow was subsequently employed. Initially, the SelectIntegrationFeatures function was used to identify genes exhibiting consistent variability. Following this, the FindIntegrationAnchors function identified a set of anchors between the human and porcine datasets by leveraging the top 30 dimensions from the canonical correlation analysis to define the neighbor search space.

This process facilitated the generation of an integrated dataset using the `IntegrateData` function. Post-integration, cell cycle effects were regressed out, and clustering analysis was conducted via a series of functions: `RunPCA`, `FindNeighbors`, `FindClusters`, and `RunUMAP`. To identify differentially expressed genes (DEGs) conserved across datasets, the `FindConservedMarkers` function was employed. Further analysis was performed to pinpoint species-specific DEGs within selected clusters. An additional column was added to the Seurat object to categorize each cluster by species origin. Relevant clusters were then examined for DEGs using the `FindMarkers` function. Finally, genes displaying differential expression due to dataset-specific effects or those detected in only one species were excluded from the analysis.

Marker selection for common cell types

Markers for each of the common cell types were obtained by comparing a certain cell type with all other cell types using the binomial likelihood test embedded in the R package Seurat. In addition, we selected genes that have been published as cell-specific markers.

Differential expression analysis and gene ontology enrichment analysis

The Wilcoxon rank sum test was used to compare the expression value of each gene in a given cluster against that of the remaining genes to identify significantly upregulated genes. Genes with an adjusted *p* value less than 0.05 were considered differentially expressed genes (DEGs). We subsequently used the R package `clusterProfiler` and the annotation R package `org.Hs.eg.db` to perform Gene Ontology analysis.

Trajectory analysis

In this study, `monocle` was used for trajectory construction and pseudotemporal analysis [26]. The gene expression matrix generated by 10x Genomics was imported into `Monocle` to construct cell differentiation trajectories and visualize cell trajectories for different clusters. `Monocle` can find genes that are differentially expressed between different clusters and assess the statistical significance of those changes. We identified key genes related to the development and differentiation process with $FDR < 1e-5$ and grouped genes with similar trends in expression.

Cell communication

To investigate potential interactions across nasal cell types, `CellPhoneDB` was used to infer that cell–cell communication is mediated by ligand–receptor interactions. Among them, only receptors and ligands expressed in more than a user-specified threshold percentage of the

cells in the specific cluster were considered for the analysis (default is 10%). To identify biological relevance, we further used `CellPhoneDB` software to perform pairwise comparisons between common cell types and analysed the number of significantly enriched ligand–receptor interactions between two cell types. We defined a *P* value less than 0.05 as significant.

Cell type distribution of gene expression

The `ggplot` function of the `ggplot2` package in R was used to display the expression of respiratory virus receptors, cell–cell junction genes, and pattern recognition receptors in all epithelial cell types.

Histological analysis

The specific method used was described previously [27]. In brief, all the animals were euthanized by intravenous injection of pentobarbital sodium (100 mg/kg). The entire nasal region of each animal was subsequently removed, and the skin and muscles around the nose were peeled off. The nasal tissue was fixed in 4% paraformaldehyde stationary solution for 48 h. After fixation, five cross-sectional blocks were selected according to the nasal anatomy of pigs [4] and dehydrated with a graded alcohol series (75%, 85%, 95%, 100%, 100% ethanol). The dehydrated blocks were then embedded in paraffin, serially sliced into 5- μ m-thick sections, and mounted on slides. The slices were dried overnight at 37 °C. A cross section of the nasal respiratory region was stained with haematoxylin–eosin (HE). Integral images were scanned via a BX51 Digital Camera System (Olympus Inc., Tokyo, Japan).

Immunofluorescence staining and confocal microscopy

To show the distribution of ciliated cells, basal cells and goblet cells in porcine nasal tissue, tissue sections were rinsed and subjected to antigen repair. After being washed with PBS, the sections were treated with 3% hydrogen peroxide solution and incubated at room temperature in the dark for 15 min. Then, the sections were blocked with 5% bovine serum albumin for one hour at 37 °C and incubated with rabbit KRT5 antibody. The sections were subsequently incubated with anti-rabbit HRP secondary antibodies at room temperature for 1 h and then with FITC-TSA. For antigen repair, the sections were labelled with an anti-mouse Alexa Fluor 549 secondary antibody (alpha-Tubulin (acetyl K40)) and an anti-mouse Alexa Fluor 633 secondary antibody (MUC5AC) in sequence according to the above steps. The nuclei were stained by incubation with diamidino-2-phenylindole for

10 min and observed under a confocal laser microscope (LSM-710; Zeiss, Oberkochen, Germany).

Results

Single-cell transcriptional landscape of porcine nasal mucosal cells

To analyse the cellular composition of porcine nasal tissue in detail, nasal mucosa samples were collected and dissociated into single-cell suspensions for scRNA-seq. After quality control (including the number of genes, number of mRNA, proportion of mitochondrial gene expression, and multiple filtering), a total of 17 201 cells were obtained (Additional files 1, 2). By tSNE mapping and unsupervised density clustering, these cells were identified as 19 distinct cell types, a classification informed by the differential expression of cell-specific marker genes, as depicted in Figures 1A and B.

First, nine types of epithelial cells were identified on the basis of the expression of cell-specific marker genes. Basal cells, characterized by high expression of KRT5, TP63, and DLK2 [7], serve as tissue-specific stem cells of the airway epithelium. Suprabasal cells exhibit low levels of KRT5 and TP63, along with increasing gradients of KRT4 expression [7, 28]. Cycling basal cells were observed with elevated expression of MKI67 and TOP2A [7]. Secretory cells (including club cells and goblet cells) are found in the nasal mucosa and specifically express SCGB1A1 and MUC5AC [7]. Ciliated cells specifically express FOXJ1 and TPPP3 [7]. Notably, a rare cell type, the ionocyte type, is characterized by high levels of CFTR and FOXI1 expression [29]. Furthermore, three distinct cell types are related to sub-mucosal glands: serous cells (which express high levels of LTF and PEBP4 [7]), mucous cells (which express high levels of MYH11 and TAGLN [30]), and duct cells (which express high levels of ALDH1A3 and SOX9 [31, 32]). Next, five types of stromal cells were identified on the basis of the expression of cell-specific marker genes. These include fibroblasts (COL1A1, COL6A1, and DCN [7, 33]), endothelial cells (VWF, PECAM1, and CDH5 [9, 33]), lymphatic endothelial cells (PROX1 and FLT4 [34, 35]), smooth muscle cells (CALD1 and DES [7, 36]), and erythroid cells (HBM and HBB [37]).

In addition to these cells, various immune cell types were identified according to the expression of cell-specific marker genes. In brief, dendritic cells and macrophages exhibit increased expression of CD80, CD86, CD163 and HLA-DRA [38–40]. Natural killer cells exhibit high expression levels of NKG7, SAMD3, and GNLY [40–42], whereas T cells are enriched in CD3D and CD3E [42]. Neutrophils display high expression of SELL and CSF3R [43], and B cells are identified by the enrichment of CD19, CD79A, and PAX5 [7, 44].

Distribution characteristics of porcine nasal epithelial cells

The results of scRNA-seq revealed that basal cells, goblet cells, and ciliated cells are the three main subtypes of epithelial cells. Therefore, we focused on the distribution characteristics of these epithelial cells in porcine nasal mucosa. HE staining revealed notable variations in the morphology and structure of the porcine nasal mucosa at different anatomical sites, resulting in the subsequent division of the nasal mucosa into six distinct regions (a-f) (Figure 2A). The upper regions (a-d) of the nasal mucosa were entirely covered by pseudostratified columnar ciliated epithelia, whose cilia were long and dense. However, the cilia located in the lower regions (e-f) of the nasal mucosa were short and sparse. Moreover, the epithelial layers in regions a and f were relatively thin and consisted of approximately three layers of cells, whereas the epithelial layers in regions b, c, d and e were relatively thin and consisted of approximately five layers of cells (Figure 2A). Immunofluorescence results revealed that acetylated α -tubulin+ciliated cells were widely distributed across the epithelial surface. KRT5+basal cells were evenly distributed at the base of the epithelium. Interestingly, MUC5AC+goblet cells were exclusively identified in the lower regions of the nasal mucosa and ranged in size and shape (Figure 2B).

Differences in the composition of porcine and human nasal epithelial cells

The physiological similarities between pigs and humans are close enough to make pigs promising xenotransplant donors. However, there is still a lack of relevant research on whether there is consistency in the composition and function of nasal mucosal cells between pigs and humans. Therefore, a comparative analysis of epithelial cell populations was conducted by integrating our own data with accessible single-cell RNA sequencing data from humans. Our findings revealed that eight distinct types of epithelial cells, including basal cells, suprabasal cells, cycling basal cells, secretory cells (goblet cells and club cells), ciliated cells, serous cells, mucous cells and ionocytes, are conserved between porcine and human nasal mucosa. Notably, deuterosomal cells, which are believed to be progenitors of ciliated cells, exist only in the human nasal mucosa. Duct cells were specifically observed in the porcine nasal mucosa. The differential expression of epithelial marker genes in porcine and human nasal mucosa was subsequently analysed. The results revealed high similarity in marker gene expression between porcine and human nasal epithelial cells, such as

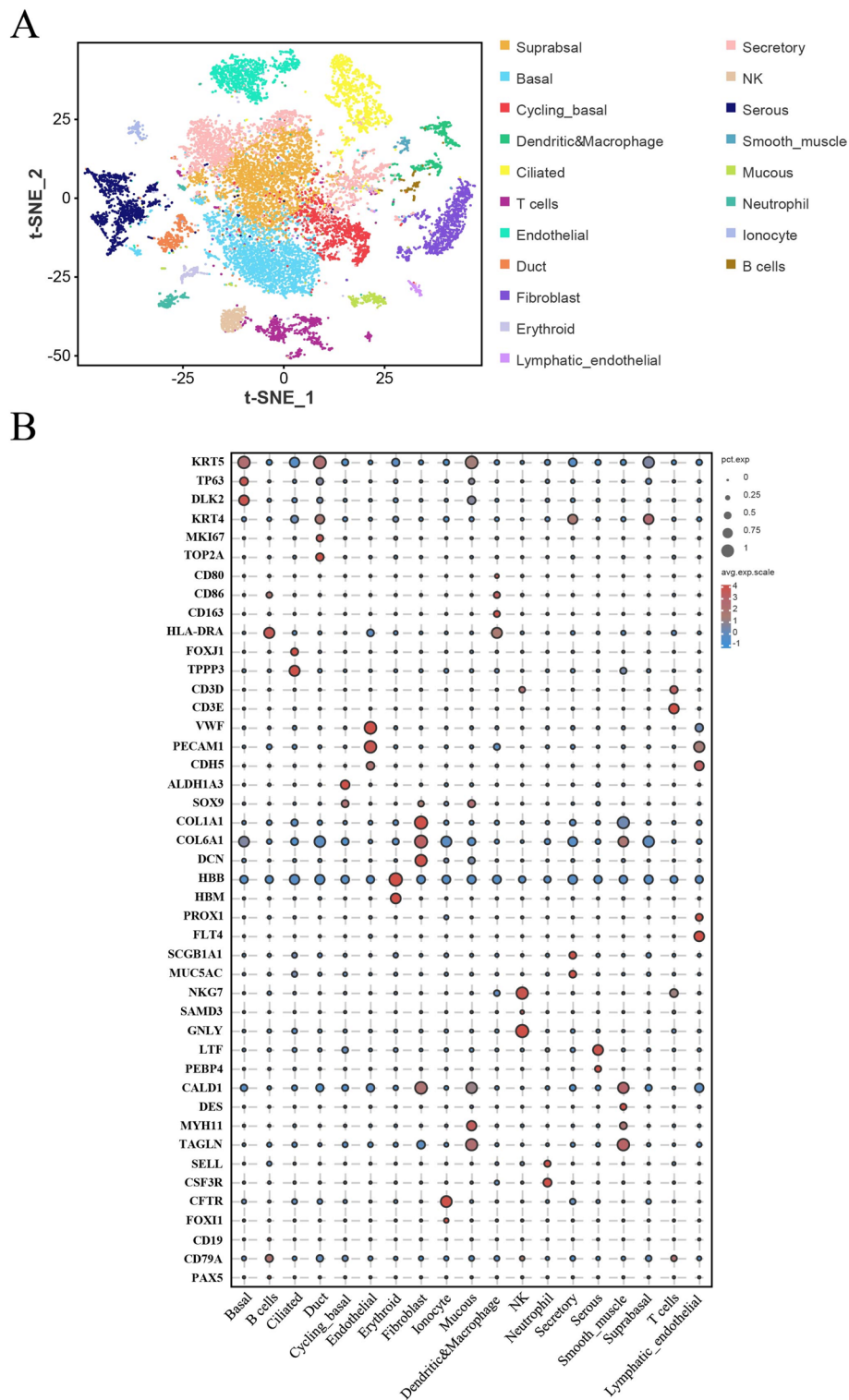


Figure 1 Single-cell atlas of the porcine nasal mucosa. **A** t-Stochastic neighbor embedding (tSNE) plots displaying 17 201 cells from porcine nasal mucosa identified as 19 distinct cell types. **B** Dot plots showing marker genes for nasal cell types, with the fraction of expressing cells and average expression within each cell type indicated by dot size and color, respectively.

KRT5 for basal cells and FOXJ1 for ciliated cells. In addition, we screened several unique molecular markers that are expressed in porcine epithelial cells, such as BEST4 for human ciliated cells and DPEP2 for porcine ciliated cells (Figures 3A and B).

To determine whether the function of nasal epithelial cells is conserved between pigs and humans, a Gene Ontology (GO) enrichment analysis of biological processes was conducted. The identical cell types in both pigs and humans presented very similar patterns of enriched pathways (data not shown), with the exception of secretory cells. In porcine nasal secretory cells, the enriched GO terms were predominantly associated with biological reactions, such as response to chemical, response to cytokine, immune response, and response to stimulus (Figure 3C). However, the enriched GO terms in human nasal secretory cells were related primarily to material transport processes, including transport, vesicle-mediated transport, exocytosis, and regulated exocytosis (Figure 3D). Moreover, we focused on the biological functions of porcine duct cells and found that the enriched GO terms in porcine duct cells were always associated with energy metabolism, such as cellular respiration and ATP metabolic processes (Figure 3E).

In terms of immune cells, T cells, dendritic cells, and macrophages are present in both porcine and human nasal mucosa. However, porcine nasal mucosa contains a greater diversity of immune cell types, including NK cells, neutrophils, and B cells.

Pseudotime analysis of porcine and human nasal epithelial cell development

To investigate the differences in the differentiation process of nasal epithelial cells between pigs and humans, the Monocle tool was employed to reconstruct differentiation trajectories via the pseudotemporal ordering of single cells. The differentiation trajectories of porcine and human nasal epithelial cells exhibited the same trend. Specifically, basal cells, which then differentiate into club cells and further differentiate into ciliated cells or goblet cells, are used as a starting point for nasal epithelial cell differentiation (Figures 4A–D).

A thorough analysis of the dynamics of transcription factors during the development of nasal epithelial cells was subsequently performed. In both pigs and humans, genes associated with the differentiation and development of epithelial cells, such as JAG1, TGFB1, BMP7 and WNT10A, as well as those involved in cell adhesion, such as SNAI2, presented significant expression levels in the early stages. In contrast, certain genes associated with epithelial cell differentiation and development presented increased expression in the later stages in pigs but were more prominent in the early stages in humans

(Figures 4E and F). These findings indicate a degree of conservation in the transcription factors responsible for regulating nasal epithelial cell differentiation in both pigs and humans.

Cell-cell communication between porcine and human nasal epithelial cells

CellPhoneDB was used to explore the cell–cell interactions between nasal epithelial cells and identify significantly enriched ligand–receptor pairs. This analysis revealed a greater level of ligand–receptor interaction in porcine nasal epithelial cells than in human nasal epithelial cells (Figures 5A and B). Specific interactions between basal cells and cycling basal cells almost invariably involve processes related to proliferation and differentiation, such as EGFR-TGFB1, EGFR-MIF, and DAG1-LGALS9 in pigs and humans; FZD6-WNT, TGFB3-TGFB1, and NGFR-NTF3 in pigs; and EPHB4-EPNB1 and LRP1-MDK in humans. In addition, we identified interactions related to the maintenance of epithelial integrity (NECTIN1-NECTIN3) in pigs (Figure 5C). Similarly, the interactions between suprabasal cells and secretory cells are significantly correlated with proliferation and differentiation. Specifically, NOTCH2-JAG1 and EPHB2-EPNB1 were enriched in both pigs and humans, whereas EPGB4-EPNB1 was enriched exclusively in pigs, and CD74-COPA and EGFR-MIF were enriched exclusively in humans (Figure 5D). These findings suggest that the regulation of nasal epithelial cell development in both pigs and humans involves a combination of conserved and species-specific interactions.

Transcription characteristics of cell–cell junction molecules and pattern recognition receptors in porcine and human nasal epithelial cells

Cell–cell junctions and pattern recognition receptors (PRRSs) are important parts of the innate immune system. This study examined the expression patterns of genes associated with cell–cell junction molecules and pattern-recognition receptors in nasal epithelial cells of both pigs and humans. A significant proportion of genes related to cell–cell junctions presented similar expression profiles across these two species. Specifically, JAM2, JAM3, and CLDN5 presented minimal expression levels in the majority of nasal epithelial cell types. Conversely, CLDN1, NECTIN1, AFDN, TJP1, and TJP3 were highly expressed in most nasal epithelial cell types of both pigs and humans (Figures 6A and B).

However, the expression patterns of PRRS significantly differ between porcine and human nasal epithelial cells. Our analysis revealed that the mRNA transcripts of TLR6, TLR8, TLR9, TLR10, and NLRC3, which are present at low levels in porcine nasal

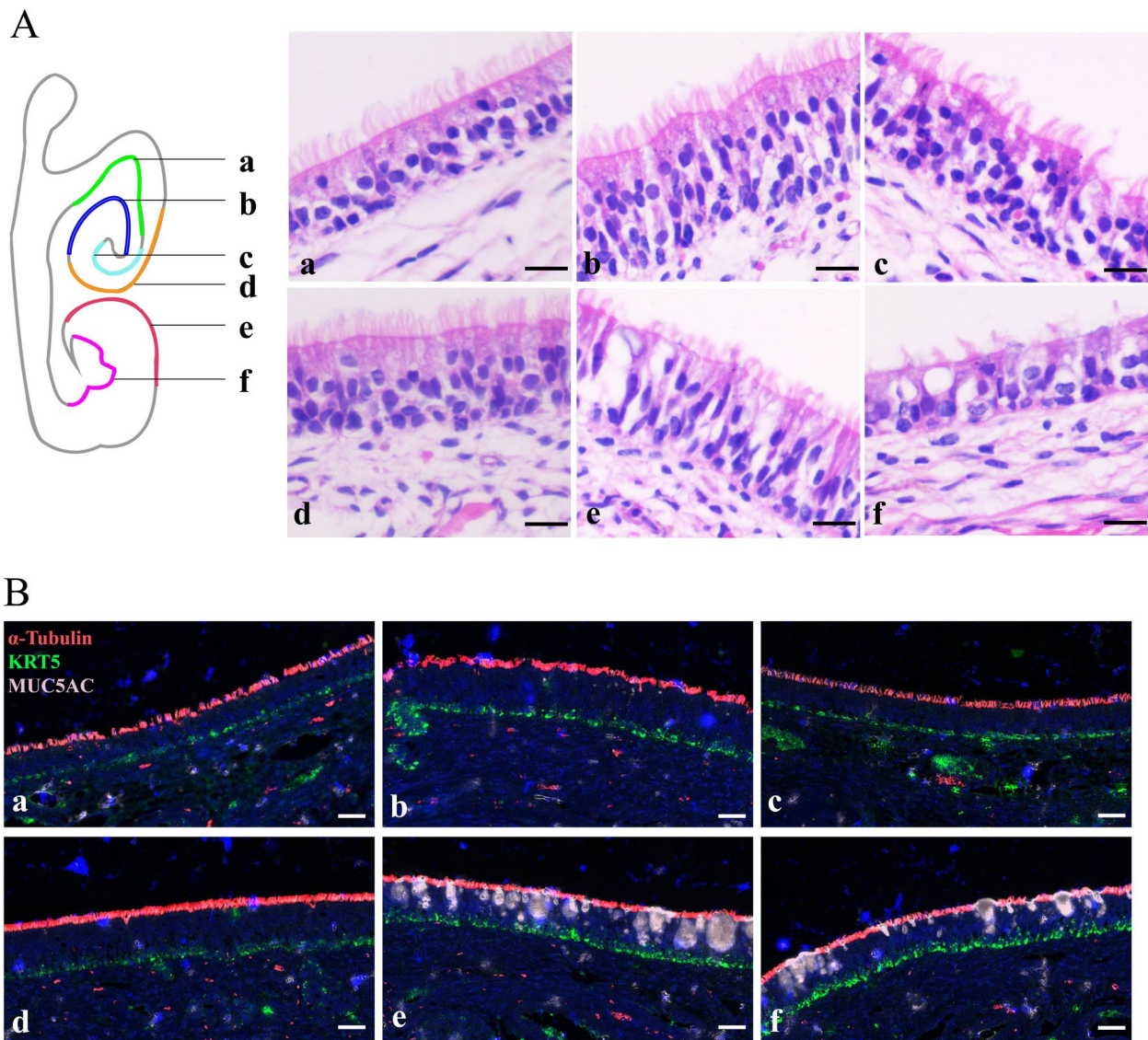


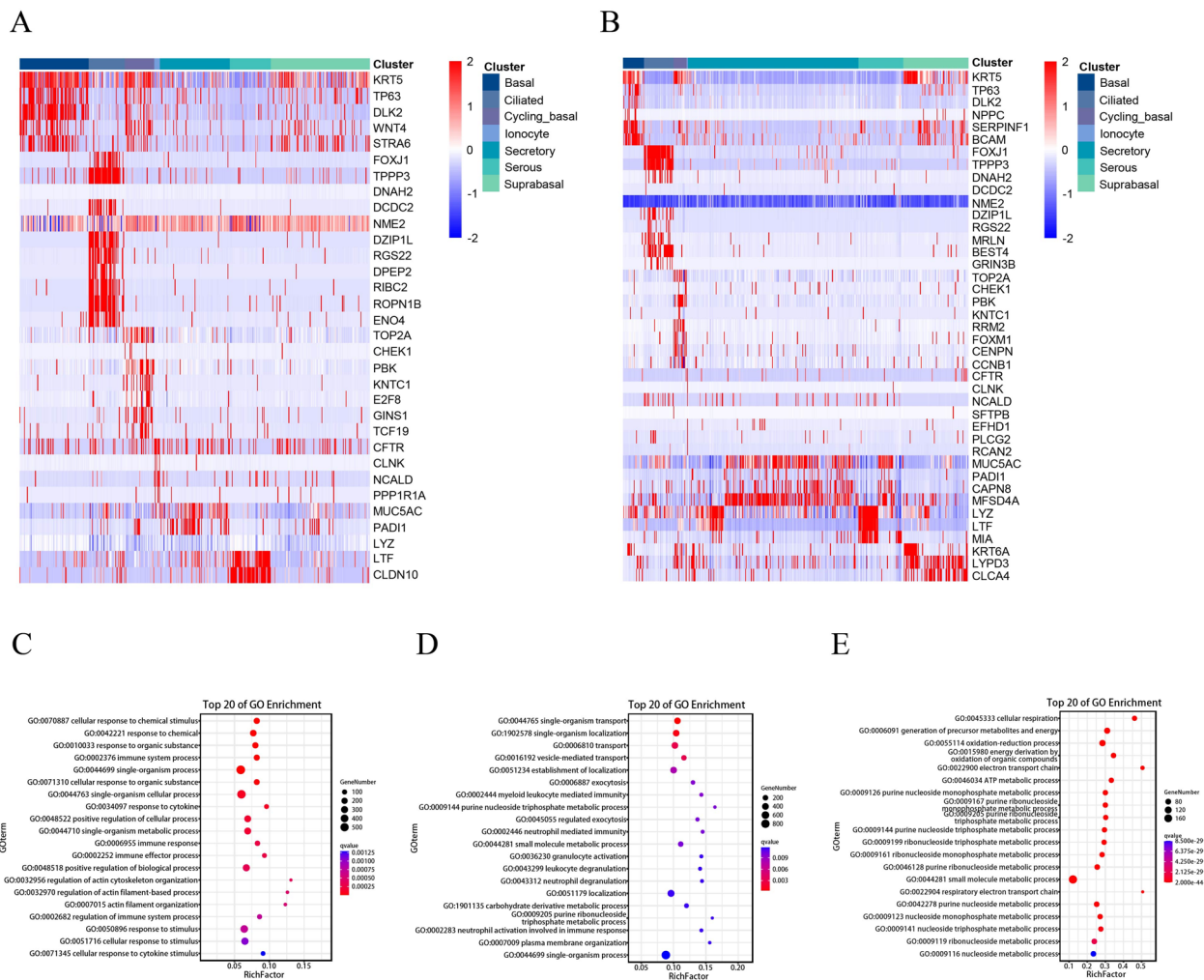
Figure 2 Morphological characteristics and basal, ciliated, and goblet cell distributions of porcine nasal mucosa. **A** The nasal mucosa was separated into six distinct areas (a-f). HE staining of different areas of the pig nasal concha. Scale bars: 10 μ m. **B** Immunofluorescence staining for KRT5 (green, representing basal cells), acetylated α -tubulin (red, representing ciliated cells), and MUC5AC (pink, representing goblet cells) in the pig nasal concha. Nuclei are shown in blue (DAPI). Scale bars: 20 μ m.

epithelial cells, were absent in human nasal epithelial cells (Figures 6C and D). Additionally, TLR3 and TLR4 exhibited high mRNA levels across various porcine epithelial cell types (Figure 6C), whereas CLEC7A and NLRC5 presented high expression in most human epithelial cell types (Figure 6D). By comparing the expression levels of PRRs in nasal epithelial and innate immune cells (dendritic cells and macrophages), we found that almost all PRRs (except TLR3) had higher expression levels in porcine nasal innate immune cells than in epithelial cells (Figure 6C). In human nasal epithelial cells, TLR1, TLR2, TLR4, TLR7, and CLEC7A

presented relatively high expression levels, whereas TLR3, NLRC5, DDX58, IFIH1, and DHX58 were highly expressed in human nasal innate immune cells (Figure 6D).

Transcriptional characteristics of respiratory virus receptors in porcine and human nasal epithelial cells

The nasal cavity serves as a primary site of entry for respiratory viruses, making it an important target for infection. In this study, the distribution of the expression of multiple respiratory virus receptors in porcine and human nasal epithelial cells was examined. Our



findings indicated that most respiratory virus receptors display similar expression profiles across different cell types in both porcine and human nasal epithelial cells (Figure 7A and B, Additional file 4). Specifically, receptors such as ANXA5, EGFR, and ITGB1 were widely expressed across various nasal epithelial cell types in both species (Figure 7C and D). ITGA5 and ASGR1 exhibited significantly low expression levels in all nasal epithelial cell types of both species (Additional file 3). In addition, species-specific differences in the expression of certain virus receptors were detected. Specifically, ANPEP and LDLR were found to have low expression levels in all porcine nasal epithelial cell types but were prominently detected in

most human nasal epithelial cell types, particularly secretory cells (Additional file 3). DPP4 was found to be present in a limited number of human nasal epithelial cell types, whereas it was notably abundant in the majority of epithelial cell types in pigs. ACE2 exhibited extremely low mRNA expression in human nasal epithelial cells and was virtually absent in porcine nasal epithelial cells (Additional file 3). Notably, CD46 was expressed solely in human nasal epithelial cells, whereas RTN4R, CX3CR1, ITGB3, CD209, and SLAMF1 were uniquely expressed in porcine nasal epithelial cells (Figures 7A and B). Moreover, ciliated cells presented the highest abundance of viral receptor

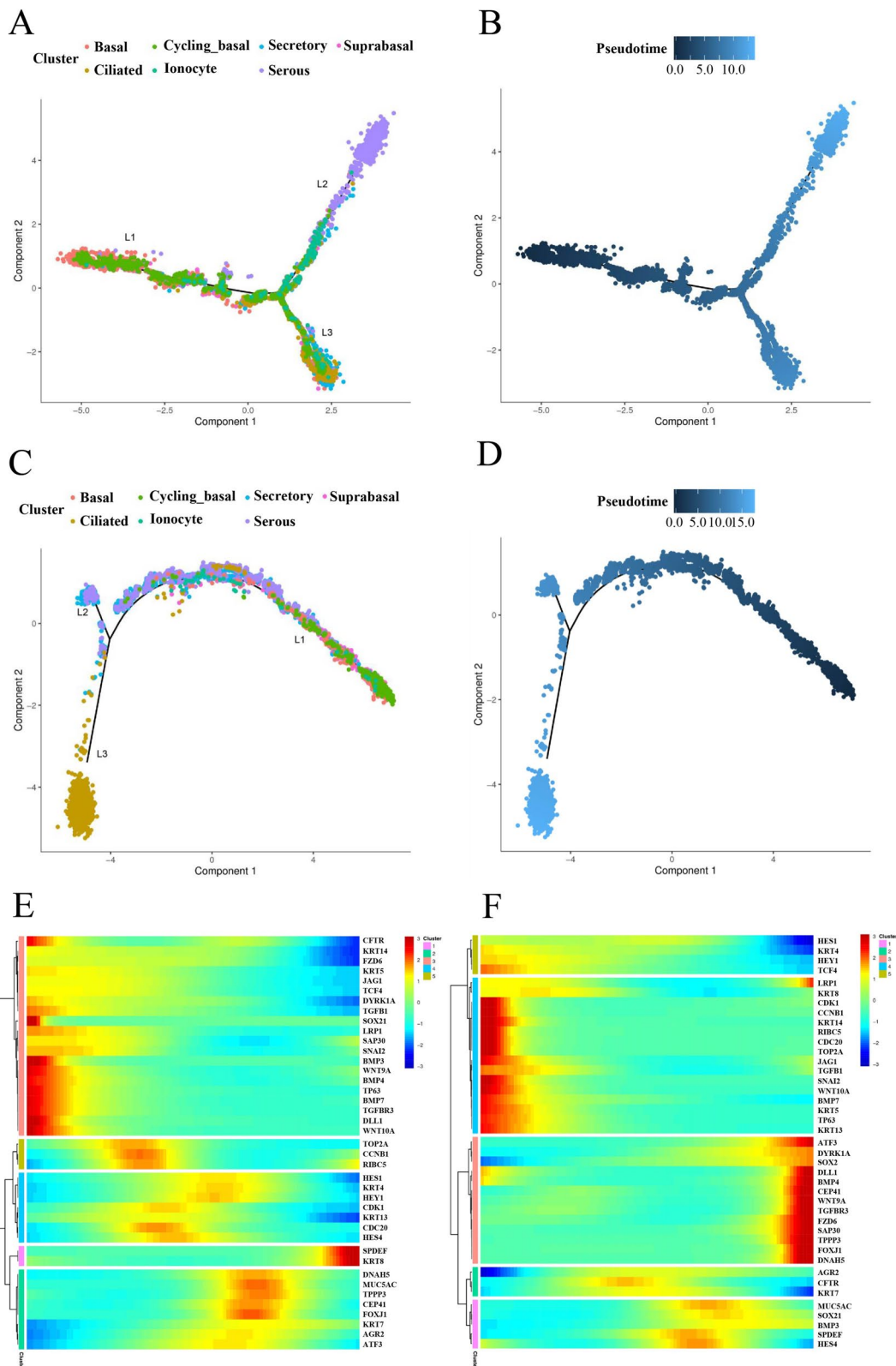


Figure 4 Pseudotime analysis of porcine and human nasal epithelial cell development. **A, B** Differentiation trajectory of porcine nasal epithelial cells, with each point coloured according to epithelial cell type (**A**) and pseudotime (**B**). **C, D** Differentiation trajectory of human nasal epithelial cells, with each point coloured according to the epithelial cell type (**C**) and pseudotime (**D**). **E, F** The gene expression levels along the pseudotime trajectories are shown in a heatmap, and representative genes are listed. (**E**) Fig. (**F**) Human.

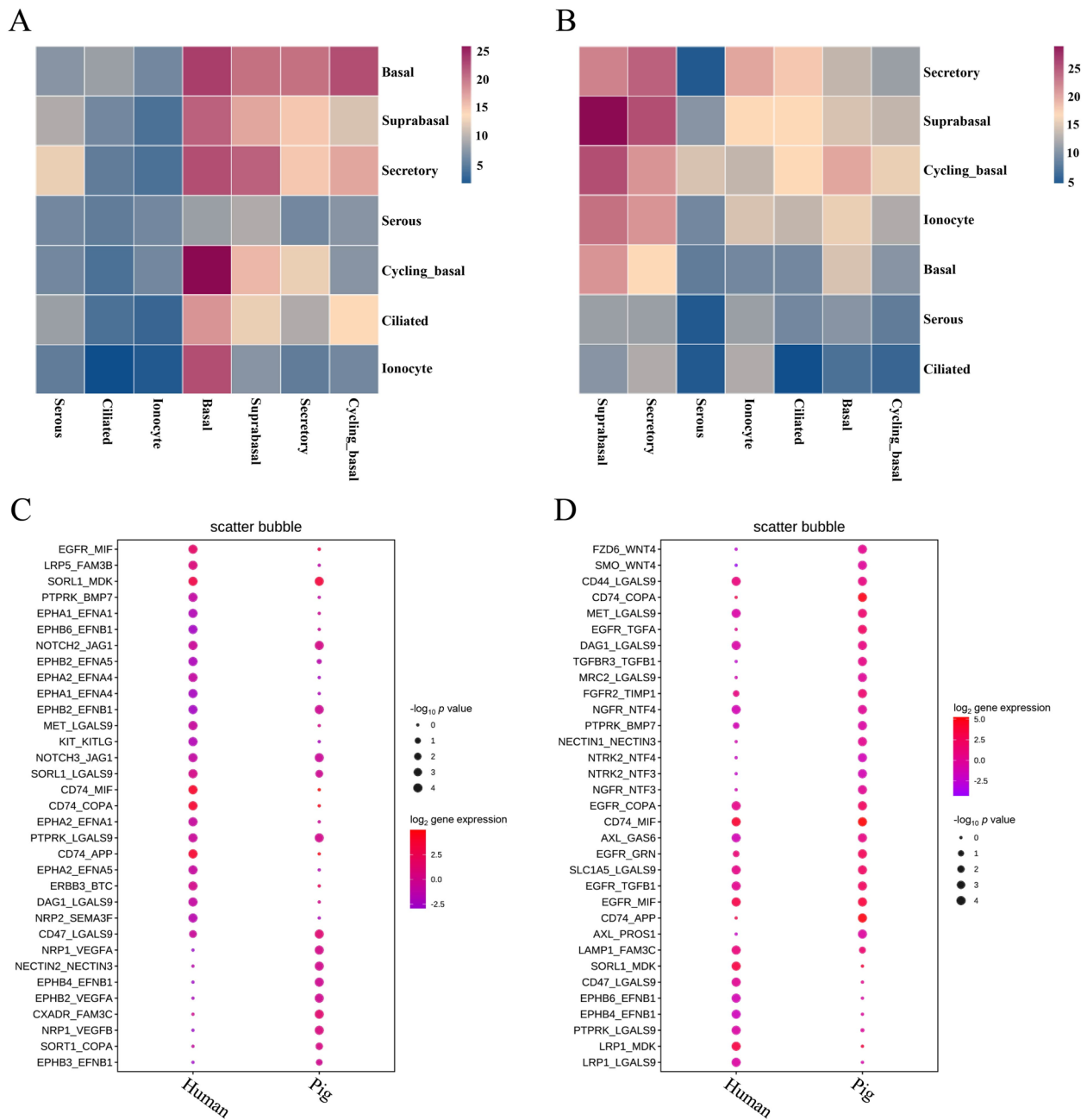


Figure 5 Cell–cell communication in nasal epithelial cells between pigs and humans. **A, B** Number of predicted interactions ($P \leq 0.05$) between nasal epithelial cells based on CellPhoneDB in pigs (**A**) and humans (**B**). **C** Predicted interactions between basal cells and cycling basal cells, comparing humans and pigs. **D** Predicted interactions between suprabasal cells and secretory cells, comparing humans and pigs.

expression compared with other types of nasal epithelial cells (Figure 7A and B).

Discussion

Exploring the cellular composition and intercellular interactions of the respiratory mucosa is essential for understanding its defense mechanisms and developing targeted therapeutic strategies [45]. In this study, we performed scRNA-seq on porcine nasal mucosa and generated a single-cell atlas comprising 17 201 cells, which were

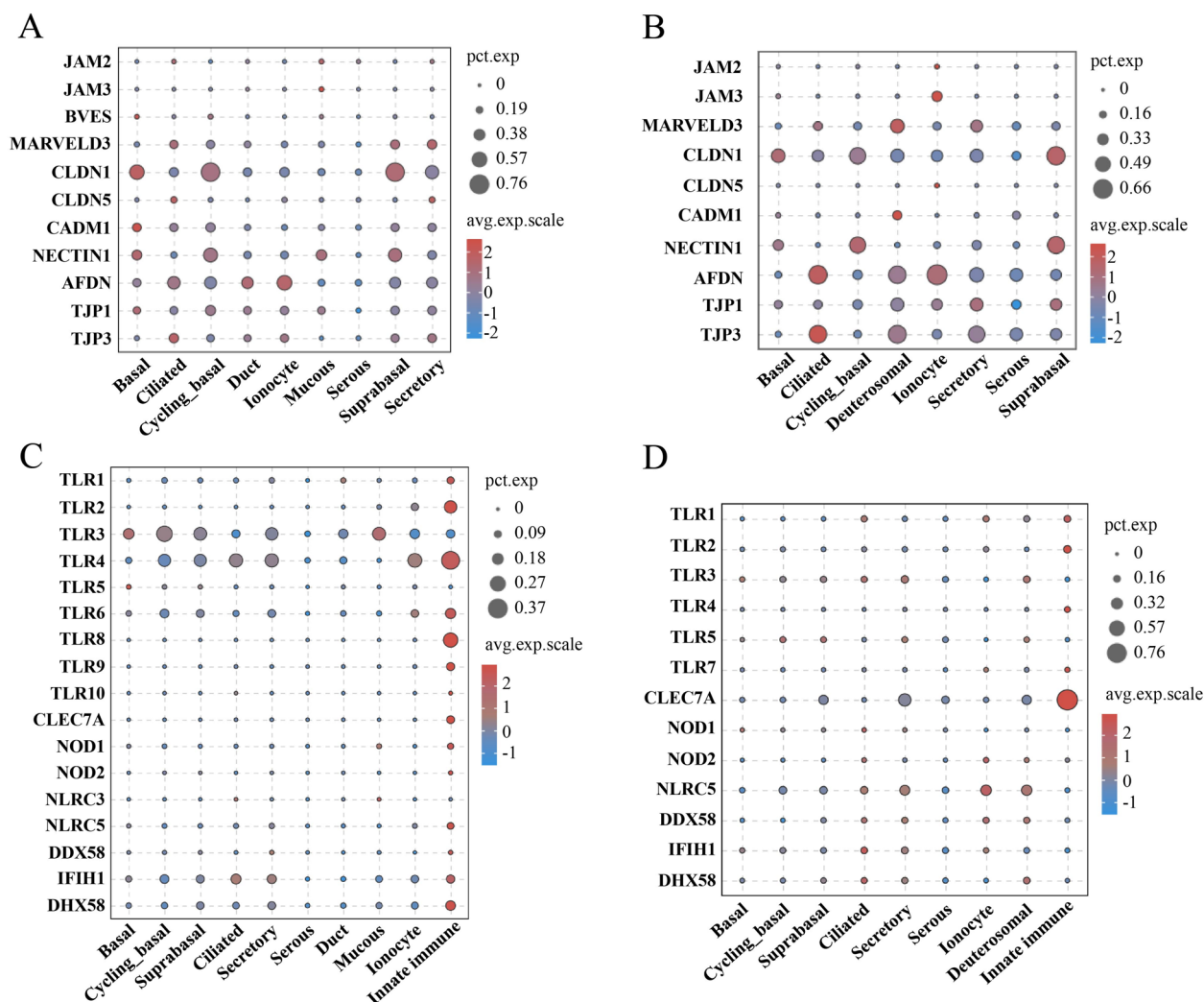


Figure 6 Expression patterns of cell–cell junction genes and pattern recognition receptors in porcine and human nasal epithelial cells. **A, B** Bubble plot showing the cell–cell junction gene expression patterns of epithelial cell types in porcine (**A**) and human (**B**) nasal tissue. **C, D** Bubble plot showing the pattern-recognition receptor expression patterns of epithelial cell types and innate immune cells (dendritic cells and macrophages) in porcine (**C**) and human (**D**) nasal regions. The size represents the percentage of cells, and the colour indicates the average scaled expression level.

identified as 19 distinct cell types, including nine epithelial cell types, five stromal cell types, and five immune cell types. The distribution characteristics of the three most representative epithelial cells in the porcine nasal mucosa were subsequently depicted. Our analysis revealed that basal cells and ciliated cells are evenly distributed across the entire mucosal epithelial layer. Ciliated cells, which mediate the mucociliary clearance process, play a critical role in expelling particles and pathogens [46]. Basal cells function as tissue-specific stem cells in the airway, are crucial for long-term self-renewal and are vital for maintaining and repairing the respiratory epithelium [47, 48]. The strategic distribution of ciliated cells and basal cells

likely contributes to reducing pathogen colonization and aids in maintaining homeostasis. In contrast, the distribution of goblet cells showed significant regional specificity, which predominated in the lower but was scarce in the upper regions of the porcine nasal mucosa. Considering that goblet cells are responsible for mucus production and that mucus serves as a key component of the mucosal defense mechanism against microbial invasion [49, 50], this uneven distribution suggests potential increased vulnerability to pathogen infection in upper mucosal regions.

Although domestic pigs are generally believed to share histological similarities with humans [51], existing studies

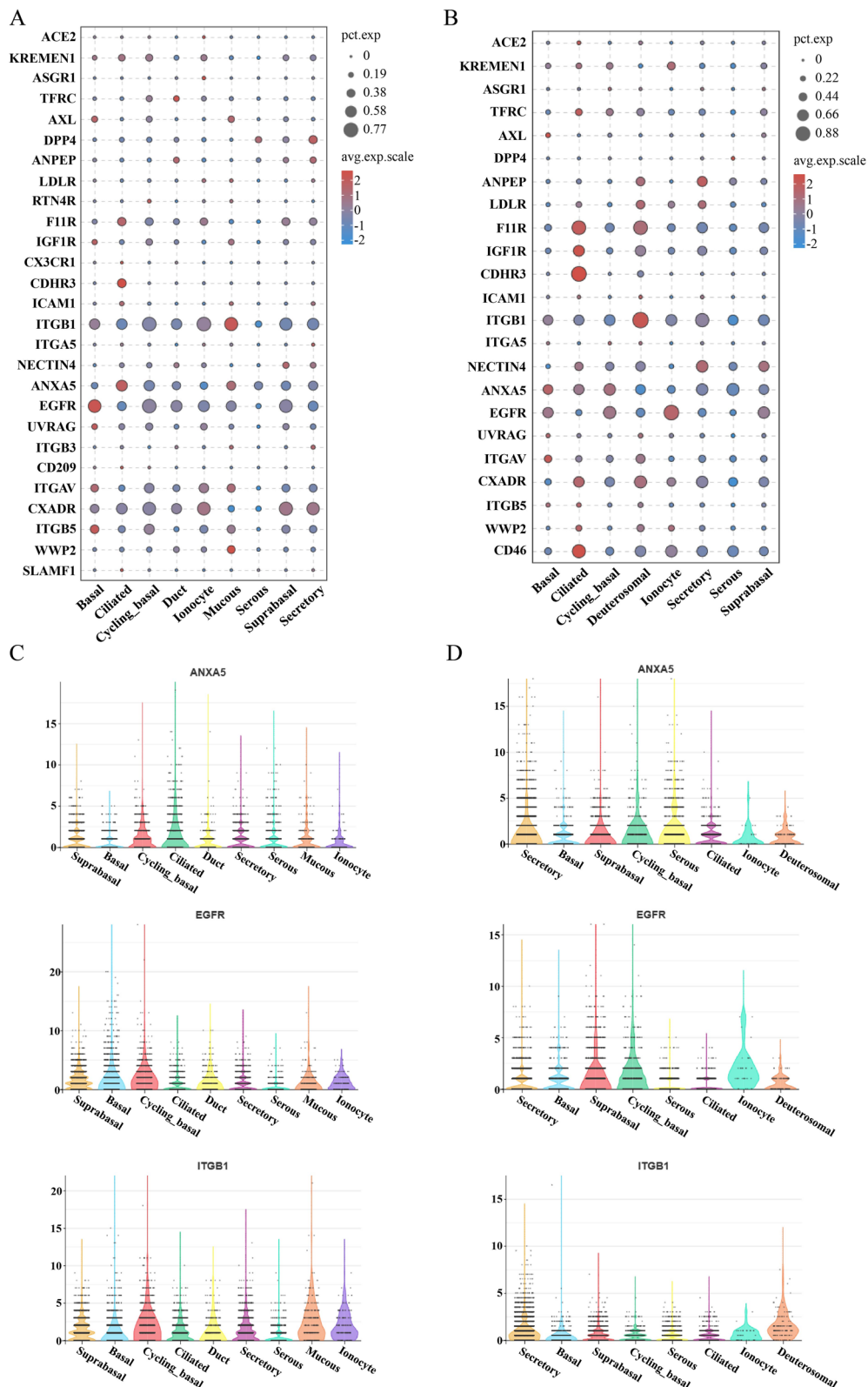


Figure 7 Expression patterns of respiratory virus receptors in porcine and human nasal epithelial cells. **A, B** Bubble plot showing the virus receptor expression patterns of epithelial cell types in pig (**A**) and human (**B**) nasal regions. The size represents the percentage of cells, and the colour indicates the average scaled expression level. **C, D** Violin plots showing the expression of ANXA5, EGFR, and ITGB1 in porcine nasal (**C**) and human nasal (**D**) samples.

have yet to compare the cellular composition and transcriptional characteristics of porcine and human nasal mucosa effectively. Our study revealed that both porcine and human nasal epithelia consist of basal cells, suprabasal cells, cycling basal cells, club cells, goblet cells, ciliated cells, ionocytes, serous cells and mucous cells. Moreover, the marker genes of these nasal epithelial cells are highly conserved between pigs and humans. These findings suggest that the functional roles of the nasal epithelium are likely similar across these two species. Duct cells, which are commonly found in the pancreas, have also been identified in the porcine nasal cavity and exhibit robust energy metabolism activity. Given their role in the secretion of mucin and fluid/electrolytes, particularly HCO_3^- [52–54], the presence of these cells in the porcine nasal cavity may enhance the functional role of the mucosal barrier, meriting further investigation. There is a notable difference in the composition of immune cells in the nasal mucosa between humans and pigs. Given that nasal immune cells are located primarily in the submucosal lamina propria [5], the observed differences may be attributable to the sampling method employed.

Pseudotime analysis, also known as trajectory inference, is used to infer the differentiation trajectory of cells or the evolution process of cell subtypes [55, 56]. Our pseudotime analysis revealed that the differentiation trajectories of nasal epithelial cells in pigs and humans are remarkably similar; both start with basal cells, progress to club cells, and then branch into either ciliated cells or goblet cells under the regulation of different transcription factors. Signalling pathways such as the Notch, Wnt, and BMP/TGF β pathways play important roles in nasal epithelium development [57]. Our results revealed that the expression patterns of key transcription factors within these pathways (such as JAG1, TGFB1, BMP7 and WNT10A) are similar in both porcine and human nasal epithelial cells. These findings indicate the conserved development of nasal epithelial cells across pigs and humans.

Interactions between cellular populations are essential for the development of the nasal mucosa and the maintenance of the mucosal barrier [58]. Our study revealed that the ligand-receptor pairs between nasal epithelial cells in pigs and humans, such as EGFR-TGFB1, EGFR-MIE, TGFBR3-TGFB1, NGFR-NTF3, EPHB4-EPHB1 and LRP1-MDK, are related to epithelial development [59, 60]. However, the expression patterns of these receptors and ligands are species specific. Taking the interaction between basal cells and cycling basal cells as an example, in pigs, the TGFBR3-TGFB1 and NGFR-NTF3 signalling pathways were specifically activated, whereas in humans, the EPHB4-EPHB1 and LRP1-MDK pathways were specifically activated. These findings suggest that

these pathways may uniquely contribute to the development of nasal epithelial cells in each species. Notably, our research also highlighted the unique activation of the NECTIN1-NECTIN3 signalling pathway in pigs, which is known to play a crucial role in forming, maintaining, and modifying cellular junctions [61]. This specific activation implies its potential involvement in establishing early epithelial barriers in pigs.

The maintenance of the physical barrier of the nasal mucosa requires the involvement of cell-cell junctions, including tight junctions, adherens junctions and desmosomes [62, 63]. The observation of similar expression patterns of these junction molecules in porcine and human nasal epithelial cells suggested that the nasal epithelia of pigs and humans have similar physical barrier functions. Pattern recognition receptors (PRRs), which detect pathogens by recognizing pathogen-associated molecular patterns (PAMPs), play a vital role in host defense mechanisms [64]. Our research revealed that pigs exhibit significantly greater variety and expression levels of pattern recognition receptors than humans do. Notably, TLR3, which targets double-stranded RNA from viruses [65, 66], and TLR4, which are activated by bacterial lipopolysaccharides [67, 68], are highly expressed in porcine nasal epithelial cells. These findings suggest that the porcine nasal mucosa may have a stronger innate immune response to infection. PRRs are involved primarily in innate immunity, and macrophages [69] and dendritic cells [70] are the main innate immune cell types. Our findings indicate that the expression levels of PRRs in porcine nasal epithelial cells are significantly lower than those in innate immune cells. These findings suggest that innate immune cells remain the primary mediators of pathogen recognition and the immune response within the porcine nasal mucosa. However, in humans, certain receptors (such as TLR1, TLR2, TLR4, TLR7, and CLEC7A) exhibit relatively high expression levels in nasal epithelial cells, suggesting that human nasal epithelial cells may have evolved a relatively strong innate immune recognition capability.

Pigs are susceptible to a variety of human respiratory pathogens. We found that multiple human respiratory virus receptors, such as ANXA5, ITGB1, ITGA5 and EGFR, exhibit similar expression patterns in porcine and human nasal epithelial cells. Among these, ANXA5 and EGFR have been identified as coreceptors for the influenza virus [71, 72]. The similar expression patterns of these two receptors in both porcine and human nasal epithelial cells may explain why pigs and humans exhibit comparable susceptibility and pathogenic responses to influenza viruses. Notably, our results revealed that ciliated cells presented the highest levels of viral receptor expression. Since ciliated cells are primary targets

for RSV and SARS-CoV-2 [73, 74], they are likely more susceptible to infections by various respiratory viruses. However, two issues need to be noted.

First, protein expression levels are crucial in determining cellular functions; thus, investigating the concordance between protein expression and transcription levels in greater detail is essential. Second, the conservation of receptors can affect ligand–receptor affinity. For example, ACE2 is a well-known receptor for SARS-CoV-2 in humans. Although pigs possess ACE2, differences in amino acid sequences and protein structures make pigs less susceptible to SARS-CoV-2 infection [75, 76]. Additionally, numerous reports indicate that protein modifications can affect the affinity between viruses and their receptors [77]. Consequently, the conservation of receptors across species significantly impacts the susceptibility of viruses.

In conclusion, our study substantially enhances the understanding of the cellular composition and gene expression profiles of the nasal mucosa of domestic pigs. By conducting a comparative analysis of single-cell data from porcine and human nasal mucosa, we identified significant parallels between porcine and human nasal epithelial cells in terms of their cellular composition, differentiation trajectories, and transcription characteristics of cell–cell junction molecules and various respiratory virus receptors. These insights provide a strong foundation for the use of porcine nasal cavities as alternative models for studying human respiratory diseases.

Supplementary Information

The online version contains supplementary material available at <https://doi.org/10.1186/s13567-024-01403-w>.

Additional file 1. Quality control of single-cell RNA sequencing. (A) Number of genes, mRNA count, and proportion of mitochondrial gene expression in single cells of each sample before filtering. (B) Number of genes, mRNA count, and proportion of mitochondrial gene expression in single cells of each sample after filtering. (C) tSNE plot of the multiplet distribution in each sample.

Additional file 2. Cell data quantities in each sample before and after filtering.

Additional file 3. Expression of respiratory virus receptors in porcine and human nasal epithelial cells. (A) Violin plots showing the expression of ITGA5 and ASGR1 in porcine nasal (left panel) and human nasal (right panel) samples. (B) Violin plots showing the expression of ANPEP and LDLR in porcine nasal (left panel) and human nasal (right panel) samples. (C) Violin plots showing the expression of DPP4 and ACE2 in porcine nasal (left panel) and human nasal (right panel) samples.

Additional file 4. The relationships between receptors and respiratory viruses.

Acknowledgements

This work was supported by the National Key Research and Development Program of China (Grant No. 2022YFD1801400), the National Natural Science Foundation of China (31930109 and 32473063), the Natural Science Foundation of Jiangsu Province (No. BK20240198), the Fundamental Research Funds

for the Central Universities (KYT2023004) to J.L., and the Priority Academic Program Development of Jiangsu Higher Education Institutions (PAPD).

Authors' contributions

WW analysed the data, prepared the manuscript, and was a major contributor to the writing of the manuscript. WW, RL and QZ participated in the experiments. YC and JQ raised the piglets and collected the samples. WW, YL and QY designed the study and revised the manuscript. All authors read and approved the final manuscript.

Availability of data and materials

The scRNA-seq data of healthy piglets' nasal mucosa are available in the GEO database with accession number GSE274334.

Declarations

Ethics approval and consent to participate

The animal protocol was approved by the University of Nanjing Agriculture University Committee on Animal Resources Committee (Permit Number: NJAULLSC2022014).

Competing interests

The authors declare that they have no competing interests.

Received: 26 April 2024 Accepted: 28 August 2024

Published online: 30 October 2024

References

- Xu Q, Zhang Y, Sun W, Chen H, Zhu D, Lu C, Yin Y, Rai KR, Chen JL, Chen Y (2022) Epidemiology and genetic diversity of PCV2 reveals that PCV2e is an emerging genotype in southern China: a preliminary study. *Viruses* 14:724
- Amorij JP, Kersten GF, Saluja V, Tonnis WF, Hinrichs WL, Slütter B, Bal SM, Bouwstra JA, Huckriede A, Jiskoot W (2012) Towards tailored vaccine delivery: needs, challenges and perspectives. *J Control Release* 161:363–376
- Yuk J, Akash MMH, Chakraborty A, Basu S, Chamorro LP, Jung S (2023) Morphology of pig nasal structure and modulation of airflow and basic thermal conditioning. *Integr Comp Biol* 63:304–314
- Yang J, Dai L, Yu Q, Yang Q (2017) Histological and anatomical structure of the nasal cavity of Bama minipigs. *PLoS One* 12:e0173902
- Li Y, Yang C, Jiang Y, Wang X, Yuan C, Qi J, Yang Q (2023) Characteristics of the nasal mucosa of commercial pigs during normal development. *Vet Res* 54:37
- Jovic D, Liang X, Zeng H, Lin L, Xu F, Luo Y (2022) Single-cell RNA sequencing technologies and applications: a brief overview. *Clin Transl Med* 12:e694
- Deprez M, Zaragosi LE, Truchi M, Becavin C, Ruiz García S, Arguel MJ, Plaisant M, Magnone V, Lebrigand K, Abelanet S, Brau F, Paquet A, Pe'er D, Marquette CH, Leroy S, Barbry P (2020) A single-cell atlas of the human healthy airways. *Am J Respir Crit Care Med* 202:1636–1645
- Ziegler CGK, Allon SJ, Nyquist SK, Mbano IM, Miao VN, Tzouanas CN, Cao Y, Younis AS, Bals J, Hauser BM, Feldman J, Muus C, Wadsworth MH, Kazer SW, Hughes TK, Doran B, Gatter GJ, Vukovic M, Taliaferro F, Mead BE, Guo Z, Wang JP, Gras D, Plaisant M, Ansari M, Angelidis I, Adler H, Sucre JMS, Taylor CJ, Lin B et al (2020) SARS-CoV-2 receptor ACE2 is an interferon-stimulated gene in human airway epithelial cells and is detected in specific cell subsets across tissues. *Cell* 181:1016–1035.e19
- Wang F, Ding P, Liang X, Ding X, Brandt CB, Sjøstedt E, Zhu J, Bolund S, Zhang L, de Rooij L, Luo L, Wei Y, Zhao W, Lv Z, Haskó J, Li R, Qin Q, Jia Y, Wu W, Yuan Y, Pu M, Wang H, Wu A, Xie L, Liu P, Chen F, Herold J, Kalucka J, Karlsson M, Zhang X et al (2022) Endothelial cell heterogeneity and microglia regulons revealed by a pig cell landscape at single-cell level. *Nat Commun* 13:3620

10. Gutierrez K, Dicks N, Glanzner WG, Agellon LB, Bordignon V (2015) Efficacy of the porcine species in biomedical research. *Front Genet* 6:293
11. Lunney JK, Van Goor A, Walker KE, Hailstock T, Franklin J, Dai C (2021) Importance of the pig as a human biomedical model. *Sci Transl Med* 13:eabd5758
12. Wolf E, Kemter E, Klymiuk N, Reichart B (2019) Genetically modified pigs as donors of cells, tissues, and organs for xenotransplantation. *Anim Front* 9:13–20
13. Cooper DK, Ekser B, Ramsoondar J, Phelps C, Ayares D (2016) The role of genetically engineered pigs in xenotransplantation research. *J Pathol* 238:288–299
14. Al-Mashhadi RH, Sørensen CB, Kragh PM, Christoffersen C, Mortensen MB, Tolbod LP, Thim T, Du Y, Li J, Liu Y, Moldt B, Schmidt M, Vajta G, Larsen T, Purup S, Bolund L, Nielsen LB, Callesen H, Falk E, Mikkelsen JG, Bentzon JF (2013) Familial hypercholesterolemia and atherosclerosis in cloned minipigs created by DNA transposition of a human PCSK9 gain-of-function mutant. *Sci Transl Med* 5:166ra161
15. Kleinwort KJH, Amann B, Hauck SM, Hirmer S, Blutke A, Renner S, Uhl PB, Lutterberg K, Sekundo W, Wolf E, Deeg CA (2017) Retinopathy with central oedema in an INS (C94Y) transgenic pig model of long-term diabetes. *Diabetologia* 60:1541–1549
16. Camacho P, Fan H, Liu Z, He JQ (2016) Large mammalian animal models of heart disease. *J Cardiovasc Dev Dis* 3:30
17. Porretti PM, Orandi BJ, Kumar V, Houp J, Anderson D, Cozette Killian A, Hauptfeld-Dolesek V, Martin DE, Macedon S, Budd N, Stegner KL, Dandro A, Kokkinaki M, Kuravi KV, Reed RD, Fatima H, Killian JT Jr., Baker G, Perry J, Wright ED, Cheung MD, Erman EN, Kraebber K, Gambin T, Guy L, George JF, Ayares D, Locke JE (2022) First clinical-grade porcine kidney xenotransplant using a human decedent model. *Am J Transpl* 22:1037–1053
18. Yang JR, Kuo CY, Yu IL, Kung FY, Wu FT, Lin JS, Liu MT (2022) Human infection with a reassortant swine-origin influenza A(H1N2)v virus in Taiwan, 2021. *Virology* 19:63
19. Chen W, Yan M, Yang L, Ding B, He B, Wang Y, Liu X, Liu C, Zhu H, You B, Huang S, Zhang J, Mu F, Xiang Z, Feng X, Wen J, Fang J, Yu J, Yang H, Wang J (2005) SARS-associated coronavirus transmitted from human to pig. *Emerg Infect Dis* 11:446–448
20. García-Nicolás O, Braun RO, Milona P, Lewandowska M, Dijkman R, Alves MP, Summerfield A (2018) Targeting of the nasal mucosa by Japanese encephalitis virus for non-vector-borne transmission. *J Virol* 92:e01091–18
21. Bertho N, Meurens F (2021) The pig as a medical model for acquired respiratory diseases and dysfunctions: an immunological perspective. *Mol Immunol* 135:254–267
22. Zhang J, Liu J, Yuan Y, Huang F, Ma R, Luo B, Xi Z, Pan T, Liu B, Zhang Y, Zhang X, Luo Y, Wang J, Zhao M, Lu G, Deng K, Zhang H (2020) Two waves of pro-inflammatory factors are released during the influenza A virus (IAV)-driven pulmonary immunopathogenesis. *PLoS Pathog* 16:e1008334
23. Stuart T, Butler A, Hoffman P, Hafemeister C, Papalexi E, Mauck WM, Hao Y, Stoeckius M, Smibert P, Satija R (2019) Comprehensive integration of single-cell data. *Cell* 177:1888–1902.e21
24. Korsunsky I, Millard N, Fan J, Slowikowski K, Zhang F, Wei K, Baglaenko Y, Brenner M, Loh PR, Raychaudhuri S (2019) Fast, sensitive and accurate integration of single-cell data with Harmony. *Nat Methods* 16:1289–1296
25. Butler A, Hoffman P, Smibert P, Papalexi E, Satija R (2018) Integrating single-cell transcriptomic data across different conditions, technologies, and species. *Nat Biotechnol* 36:411–420
26. Qiu X, Hill A, Packer J, Lin D, Ma Y, Trapnell C (2017) Single-cell mRNA quantification and differential analysis with census. *Nat Methods* 14:309–315
27. Zheng J, Lin J, Yang C, Ma Y, Liu P, Li Y, Yang Q (2023) Characteristics of nasal mucosal barrier in lambs at different developmental stages. *Dev Comp Immunol* 139:104587
28. Virtanen M, Sirsjö A, Vahlquist A, Törmä H (2010) Keratins 2 and 4/13 in reconstituted human skin are reciprocally regulated by retinoids binding to nuclear receptor RAR α . *Exp Dermatol* 19:674–681
29. Plasschaert LW, Žilionis R, Choo-Wing R, Savova V, Knehr J, Roma G, Klein AM, Jaffe AB (2018) A single-cell atlas of the airway epithelium reveals the CFTR-rich pulmonary ionocyte. *Nature* 560:377–381
30. Zhang L, Zhu J, Wang H, Xia J, Liu P, Chen F, Jiang H, Miao Q, Wu W, Zhang L, Luo L, Jiang X, Bai Y, Sun C, Chen D, Zhang X (2021) A high-resolution cell atlas of the domestic pig lung and an online platform for exploring lung single-cell data. *J Genet Genomics* 48:411–425
31. Madisson E, Oliver AJ, Kleshchevnikov V, Wilbrey-Clark A, Polanski K, Richoz N, Ribeiro Orsi A, Mamanova L, Bolt L, Elmentaite R, Pett JP, Huang N, Xu C, He P, Dabrowska M, Pritchard S, Tuck L, Prigmore E, Perera S, Knights A, Oszlanczi A, Hunter A, Vieira SF, Patel M, Lindeboom RGH, Campos LS, Matsuo K, Nakayama T, Yoshida M, Worlock KB et al (2023) A spatially resolved atlas of the human lung characterizes a gland-associated immune niche. *Nat Genet* 55:66–77
32. Peng J, Sun BF, Chen CY, Zhou JY, Chen YS, Chen H, Liu L, Huang D, Jiang J, Cui GS, Yang Y, Wang W, Guo D, Dai M, Guo J, Zhang T, Liao Q, Liu Y, Zhao YL, Han DL, Zhao Y, Yang YG, Wu W (2019) Single-cell RNA-seq highlights intra-tumoral heterogeneity and malignant progression in pancreatic ductal adenocarcinoma. *Cell Res* 29:725–738
33. Wang W, Xu Y, Wang L, Zhu Z, Aodeng S, Chen H, Cai M, Huang Z, Han J, Wang L, Lin Y, Hu Y, Zhou L, Wang X, Zha Y, Jiang W, Gao Z, He W, Lv W, Zhang J (2022) Single-cell profiling identifies mechanisms of inflammatory heterogeneity in chronic rhinosinusitis. *Nat Immunol* 23:1484–1494
34. Kuonqui K, Campbell AC, Sarker A, Roberts A, Pollack BL, Park HJ, Shin J, Brown S, Mehrara BJ, Kataru RP (2023) Dysregulation of lymphatic endothelial VEGFR3 signaling in disease. *Cells* 13:68
35. Pan Y, Wang WD, Yago T (2014) Transcriptional regulation of podoplanin expression by Prox1 in lymphatic endothelial cells. *Microvasc Res* 94:96–102
36. Kenney HM, Wu CL, Loisselle AE, Xing L, Ritchlin CT, Schwarz EM (2022) Single-cell transcriptomics of popliteal lymphatic vessels and peripheral veins reveals altered lymphatic muscle and immune cell populations in the TNF-Tg arthritis model. *Arthritis Res Ther* 24:64
37. Zhu L, Yang P, Zhao Y, Zhuang Z, Wang Z, Song R, Zhang J, Liu C, Gao Q, Xu Q, Wei X, Sun HX, Ye B, Wu Y, Zhang N, Lei G, Yu L, Yan J, Diao G, Meng F, Bai C, Mao P, Yu Y, Wang M, Yuan Y, Deng Q, Li Z, Huang Y, Hu G, Liu Y et al (2020) Single-cell sequencing of peripheral mononuclear cells reveals distinct immune response landscapes of COVID-19 and influenza patients. *Immunity* 53:685–696.e3
38. Tekguc M, Wing JB, Osaki M, Long J, Sakaguchi S (2021) Treg-expressed CTLA-4 depletes CD80/CD86 by trogocytosis, releasing free PD-L1 on antigen-presenting cells. *Proc Natl Acad Sci U S A* 118:e2023739118
39. Alvarez B, Martínez P, Yuste M, Poderoso T, Alonso F, Dominguez J, Ezquerro A, Revilla C (2014) Phenotypic and functional heterogeneity of CD169⁺ and CD163⁺ macrophages from porcine lymph nodes and spleen. *Dev Comp Immunol* 44:44–49
40. Yao C, Bora SA, Parimon T, Zaman T, Friedman OA, Palatinus JA, Surapaneni NS, Matusov YP, Cerro Chiang G, Kassar AG, Patel N, Green CER, Aziz AW, Suri H, Suda J, Lopez AA, Martins GA, Stripp BR, Gharib SA, Goodridge HS, Chen P (2021) Cell-type-specific immune dysregulation in severely ill COVID-19 patients. *Cell Rep* 34:108590
41. Liu H, Zhao R, Qin R, Sun H, Huang Q, Liu L, Tian Z, Nashan B, Sun C, Sun R (2022) Panoramic comparison between NK cells in healthy and cancerous liver through single-cell RNA sequencing. *Cancer Biol Med* 19:1334–1351
42. Peters AE, Knöpper K, Grafen A, Kastenmüller W (2022) A multifunctional mouse model to study the role of Samd3. *Eur J Immunol* 52:328–337
43. Sun HF, Li LD, Lao IW, Li X, Xu BJ, Cao YQ, Jin W (2022) Single-cell RNA sequencing reveals cellular and molecular reprogramming landscape of gliomas and lung cancer brain metastases. *Clin Transl Med* 12:e1101
44. Xiong LL, Xue LL, Du RL, Niu RZ, Chen L, Chen J, Hu Q, Tan YX, Shang HF, Liu J, Yu CY, Wang TH (2021) Single-cell RNA sequencing reveals B cell-related molecular biomarkers for Alzheimer's disease. *Exp Mol Med* 53:1888–1901
45. Matthys OB, Hookway TA, McDevitt TC (2016) Design principles for engineering of tissues from human pluripotent stem cells. *Curr Stem Cell Rep* 2:43–51
46. Whitsett JA (2018) Airway epithelial differentiation and mucociliary clearance. *Ann Am Thorac Soc* 15:S143–s148
47. Wells JM, Watt FM (2018) Diverse mechanisms for endogenous regeneration and repair in mammalian organs. *Nature* 557:322–328
48. Teixeira VH, Nadarajan P, Graham TA, Pipinikas CP, Brown JM, Falzon M, Nye E, Poulosom R, Lawrence D, Wright NA, McDonald S, Giangreco A, Simons BD, Janes SM (2013) Stochastic homeostasis in human airway epithelium is achieved by neutral competition of basal cell progenitors. *Elife* 2:e00966

49. Viennois E, Pujada A, Sung J, Yang C, Gewirtz AT, Chassaing B, Merlin D (2020) Impact of PepT1 deletion on microbiota composition and colitis requires multiple generations. *NPJ Biofilms Microbiomes* 6:27
50. Cornick S, Tawiah A, Chadee K (2015) Roles and regulation of the mucus barrier in the gut. *Tissue Barriers* 3:e982426
51. Sapozhnikov A, Gal Y, Evgy Y, Aftalion M, Katalan S, Sabo T, Kronman C, Falach R (2021) Intramuscular exposure to a lethal dose of ricin toxin leads to endothelial glycocalyx shedding and microvascular flow abnormality in mice and swine. *Int J Mol Sci* 22:12345
52. Githens S (1988) The pancreatic duct cell: proliferative capabilities, specific characteristics, metaplasia, isolation, and culture. *J Pediatr Gastroenterol Nutr* 7:486–506
53. Venglovecz V, Rakonczay Z Jr, Gray MA, Hegyi P (2015) Potassium channels in pancreatic duct epithelial cells: their role, function and pathophysiological relevance. *Pflügers Arch* 467:625–640
54. Allen A, Flemström G, Garner A, Kivilaakso E (1993) Gastroduodenal mucosal protection. *Physiol Rev* 73:823–857
55. Wang CX, Zhang L, Wang B (2022) One cell at a time (OCAT): a unified framework to integrate and analyze single-cell RNA-seq data. *Genome Biol* 23:102
56. Shulse CN, Cole BJ, Ciobanu D, Lin J, Yoshinaga Y, Gouran M, Turco GM, Zhu Y, O'Malley RC, Brady SM, Dickel DE (2019) High-throughput single-cell transcriptome profiling of plant cell types. *Cell Rep* 27:2241–2247e4
57. Ruiz García S, Deprez M, Lebrigand K, Cavard A, Paquet A, Arguel MJ, Magnone V, Truchi M, Caballero I, Leroy S, Marquette CH, Marcet B, Barbry P, Zaragosi LE (2019) Novel dynamics of human mucociliary differentiation revealed by single-cell RNA sequencing of nasal epithelial cultures. *Development* 146:dev177428
58. Kurashima Y, Kiyono H (2017) Mucosal ecological network of epithelium and immune cells for gut homeostasis and tissue healing. *Annu Rev Immunol* 35:119–147
59. Zhou T, Chen Y, Liao Z, Zhang L, Su D, Li Z, Yang X, Ke X, Liu H, Chen Y, Weng R, Shen H, Xu C, Wan Y, Xu R, Su P (2023) Spatiotemporal characterization of human early intervertebral disc formation at single-cell resolution. *Adv Sci* 10:e2206296
60. Gao S, Shi Q, Zhang Y, Liang G, Kang Z, Huang B, Ma D, Wang L, Jiao J, Fang X, Xu CR, Liu L, Xu X, Göttgens B, Li C, Liu F (2022) Identification of HSC/MPP expansion units in fetal liver by single-cell spatiotemporal transcriptomics. *Cell Res* 32:38–53
61. Hermans D, Rodriguez-Mogeda C, Kemps H, Bronckaers A, de Vries HE, Broux B (2023) Nectins and nectin-like molecules drive vascular development and barrier function. *Angiogenesis* 26:349–362
62. Zhang R, Zhang L, Li P, Pang K, Liu H, Tian L (2023) Epithelial barrier in the nasal mucosa, related risk factors and diseases. *Int Arch Allergy Immunol* 184:481–501
63. Garcia MA, Nelson WJ, Chavez N (2018) Cell-cell junctions organize structural and signaling networks. *Cold Spring Harb Perspect Biol* 10:a029181
64. Thompson MR, Kaminski JJ, Kurt-Jones EA, Fitzgerald KA (2011) Pattern recognition receptors and the innate immune response to viral infection. *Viruses* 3:920–940
65. Karimi-Googheri M, Arababadi MK (2014) TLR3 plays significant roles against hepatitis B virus. *Mol Biol Rep* 41:3279–3286
66. Chen Y, Lin J, Zhao Y, Ma X, Yi H (2021) Toll-like receptor 3 (TLR3) regulation mechanisms and roles in antiviral innate immune responses. *J Zhejiang Univ Sci B* 22:609–632
67. Zhang Y, Liang X, Bao X, Xiao W, Chen G (2022) Toll-like receptor 4 (TLR4) inhibitors: current research and prospective. *Eur J Med Chem* 235:114291
68. Aboudounya MM, Heads RJ (2021) COVID-19 and Toll-Like Receptor 4 (TLR4): SARS-CoV-2 may bind and activate TLR4 to increase ACE2 expression, facilitating entry and causing hyperinflammation. *Mediators Inflamm* 2021:8874339
69. Mukhopadhyay S, Plüddemann A, Gordon S (2009) Macrophage pattern recognition receptors in immunity, homeostasis and self tolerance. *Adv Exp Med Biol* 653:1–14
70. Balan S, Saxena M, Bhardwaj N (2019) Dendritic cell subsets and locations. *Int Rev Cell Mol Biol* 348:1–68
71. Lai KM, Goh BH, Lee WL (2020) Attenuating influenza a virus infection by heparin binding EGF-like growth factor. *Growth Factors* 38:167–176
72. Yu DS, Wu XX, Weng TH, Cheng LF, Liu FM, Wu HB, Lu XY, Wu NP, Sun SL, Yao HP (2024) Host proteins interact with viral elements and affect the life cycle of highly pathogenic avian influenza a virus H7N9. *Heliyon* 10:e28218
73. Ahn JH, Kim J, Hong SP, Choi SY, Yang MJ, Ju YS, Kim YT, Kim HM, Rahman MDT, Chung MK, Hong SD, Bae H, Lee CS, Koh GY (2021) Nasal ciliated cells are primary targets for SARS-CoV-2 replication in the early stage of COVID-19. *J Clin Invest* 131:e148517
74. Griffiths CD, Bilawchuk LM, McDonough JE, Jamieson KC, Elawar F, Cen Y, Duan W, Lin C, Song H, Casanova JL, Ogg S, Jensen LD, Thienpont B, Kumar A, Hobman TC, Proud D, Moraes TJ, Marchant DJ (2020) IGF1R is an entry receptor for respiratory syncytial virus. *Nature* 583:615–619
75. Bakhshandeh B, Sorboni SG, Javanmard AR, Mottaghi SS, Mehrabi MR, Sorouri F, Abbasi A, Jahanafrooz Z (2021) Variants in ACE2; potential influences on virus infection and COVID-19 severity. *Infect Genet Evol* 90:104773
76. Hussain M, Jabeen N, Raza F, Shabbir S, Baig AA, Amanullah A, Aziz B (2020) Structural variations in human ACE2 may influence its binding with SARS-CoV-2 spike protein. *J Med Virol* 92:1580–1586
77. Peck KM, Cockrell AS, Yount BL, Scobey T, Baric RS, Heise MT (2015) Glycosylation of mouse DPP4 plays a role in inhibiting Middle East respiratory syndrome coronavirus infection. *J Virol* 89:4696–4699

Publisher's note

Springer Nature remains neutral with regard to jurisdictional claims in published maps and institutional affiliations.